

# Chaotic Spread-Spectrum Communication: A Comparative Study between Chaotic Synchronization and Matched Filtering

Nikolajs Tihomorskis <sup>\*,1</sup>, Andreas Ahrens <sup>†,2</sup> and Arturs Aboltins <sup>‡,3</sup>

\*Institute of Photonics, Electronics and Telecommunications, Faculty of Computer Science and Power Engineering, Riga Technical University, 12 Azenes Street, LV-1048, Riga, Latvia, <sup>†</sup>Faculty of Engineering, Hochschule Wismar, University of Applied Sciences, Technology, Business and Design, Philipp-Muller-Straße 14, 23966 Wismar, Germany.

**ABSTRACT** This publication investigates the performance of demodulation methods utilized in spread spectrum chaotic communication systems in order to understand conditions at which advanced demodulation methods, such as chaotic synchronization, provide tangible benefits over classical, matched filtering-based approaches. We conduct simulations and comparisons of three different communication systems: classic direct sequence spread spectrum (DSSS), chaotic signal fragment-based pseudo-chaotic spread spectrum (PCSS), and chaotic synchronization-based antipodal chaos shift keying (ACSK). These systems possess similar spectral and time domain characteristics, allowing us to shed light on their fundamental differences and limitations in chaos-based communication. Additionally, we assess the impact of frequency modulation (FM) on these modulation methods, as FM allows the creation of simplified non-coherent modulation schemes. Our findings, based on the analysis of bit error ratio (BER) curves, demonstrate that in the case of a non-dispersive communication channel, the utilization of chaotic synchronization does not allow to achieve performance of correlation-based receivers. Additionally, the utilization of chaotic synchronization for multiple access poses certain challenges due to malicious synchronization between users. As a supplementary finding, we show that in systems with matched filter-based demodulation, discrete-time quantized spreading sequences confer an advantage over analogous, continuous-time spreading waveforms.

## KEYWORDS

Spread spectrum communication  
Chaotic communication  
Chaos  
Multiple access interference  
Correlation  
Chaotic synchronization

## INTRODUCTION

With the increasing deployments of internet of things (IoT) and other wireless services, the mutual interference between services is increasing, leading to the necessity to improve existing solutions and move to higher frequencies. Spread spectrum (SS) systems, which are widely employed in wireless sensor networks (WSNs), are robust against low signal-to-noise ratio (SNR) and poor signal propagation conditions. However, this comes at the cost of

increased frequency bandwidth, leading to the need to share frequencies among many users.

Chaotic modulation exhibits a natural resistance to multi-path propagation due to the significantly reduced cross-correlation among segments of chaotic waveforms compared to periodic signals. Additionally, it provides a method for the physical layer security considering the unpredictability of the chaotic signals. Finally, chaotic synchronization can be used to deal with multiple synchronization tasks present in any practical communication system. This paper is devoted to comparing the main detection methods employed in chaos-based spread-spectrum systems: matched filtering and chaotic synchronization. The comparison is made using analytical derivations and modeling implemented in MATLAB Simulink. The main contribution and novelty of this research are the following: Firstly, a fair comparison between well-known and experimental chaos-based communication systems, such as

**Manuscript received:** 23 January 2024,

**Revised:** 10 March 2024,

**Accepted:** 5 April 2024.

<sup>1</sup>nikolajs.tihomorskis@rtu.lv (Corresponding author)

<sup>2</sup>andreas.ahrens@hs-wismar.de

<sup>3</sup>aboltins@rtu.lv

chaotic direct sequence spread spectrum (DSSS) and antipodal chaos shift keying (ACSK) is provided in terms of noise resistance and multiple access interference (MAI). The provided unique comparison allows us to understand both technologies' similarities, differences and limitations and their suitability for different single-user and multi-user communication scenarios. In this research, we also demonstrate that employing quantized chaotic waveforms in conjunction with matched filtering-based demodulation provides significant advantages over signals with continuous amplitude.

Studies of the chaotic communication system are rooted deeply in the 1990s when significant discoveries regarding the properties of chaos-based systems were made. The majority of chaos-based communication systems employ one of two mechanisms for the demodulation of the information: matched filtering (correlation) (Parlitz and Ergezinger 1994) and chaotic synchronization (Parlitz *et al.* 1996), initially proposed in works of Parlitz *et al.* Additionally, such systems as chaotic on-off keying (COOK) (Sangeetha and Bhaskar 2020; Mesloub *et al.* 2017; Andreyev 2023) rely on the simple envelope detection of the chaotic carrier.

The case of matched filtering does not significantly differ from non-chaotic SS systems. Namely, the transmitter uses a piece of chaotic waveform or a signal derived from a chaotic waveform to spread the data bits. Typical examples of such systems are chaos-based DSSS (Hasjuks *et al.* 2022; Cai *et al.* 2021; Yuan *et al.* 2021), which usually employ discrete-time quantized binary chaotic sequences produced by the chaotic maps. In this case, the receiver usually uses a locally stored chaotic sequence for the matched filtering. Another bright example is differential chaos shift keying (DCSK) and its derivatives (Quyen 2017; Que *et al.* 2021; Ma *et al.* 2022), where pieces of discrete-time chaotic sequences are embedded into the waveform so that the receiver can use cross-correlation between adjacent fragments of the waveform, to estimate the encoded data symbol. Another system that employs matched filtering is correlation delay shift keying (CDSK) (Zhang *et al.* 2015; Mukherjee and Ghosh 2014), where reference is delayed by a certain time and super-imposed into a chaotic payload sequence. In many cases, the chaotic sequences are modified by quantization (Litvinenko and Aboltins 2016), orthogonalization (Aboltins *et al.* 2022) and essentially lose their chaotic characteristics. In all systems mentioned above, the demodulator is implemented either as finite impulse response (FIR) filter or cross-correlation followed by strobe (Litvinenko and Aboltins 2016) or energy-based (Andreyev 2023; Aboltins *et al.* 2023) detection and all these systems possess essentially similar characteristics, such as processing gain, due to nature of correlation-based demodulator. Digital matched filtering is resource-demanding because it requires a large number of multiplications.

If the locally stored sequence is used for the matching, timing synchronization at the symbol and chip levels is necessary. Rake receiver (Patel *et al.* 2015a) employing multiple branches aids synchronization and allows to benefit from maximum-ratio combining (MRC). In publication (Berber and Gandhi 2016), it was shown that binary chaotic sequences do not improve bit error ratio (BER) compared to classical spreading sequences because BER is determined solely by bit energy and correlation properties of the sequences. In research work (Liu 2019), authors propose a direct synchronization acquisition method that relies on the chaotic nature of the spreading sequence. In DCSK, the symbol synchronization is unnecessary because reference sequences are transmitted between the payload symbols.

The second group of chaos-based communication systems relies on chaotic synchronization, a natural phenomenon observable in many physical systems (Parlitz *et al.* 1996). This type of system does not need external synchronization. In systems like chaos shift keying (CSK) and its derivatives like quadrature chaos phase-shift keying (QCPSK) (Jovic 2017; Babajans *et al.* 2021), encoding of the information is based on the alternating of the chaotic waveform in a way that does not affect chaotic features of the carrier so that at receiver, the signal is recognized by the slave chaotic oscillator and observer-based synchronization takes place. For example, in ACSK (Litvinenko *et al.* 2019), the waveform is just inverted depending on the data bit value for transmission. As practical experiments have shown (Aboltins and Tihomorskis 2023), chaotic synchronization is a very robust process and can withstand noise and interference. However, special attention must be paid to generating the chaotic signals as they are not always purely chaotic (Candido *et al.* 2015). In the more advanced system proposed in (Hassan and Hammuda 2019), the parameters of the chaotic oscillator are periodically changed to increase security. The constrained Smoothed Regularized Least Square observer method is used to demodulate the rapidly changing signal. Research (Li and Wang 2017) employs drive-response-based adaptive chaotic synchronization in the Mackey-Glass system for recovering the transmitted messages. The system uses Walsh spreading codes before chaotic modulation to improve detection robustness.

In systems that employ chaotic synchronization, continuous-time, non-quantized chaotic waveforms must be used in contrast to matched-filter-based systems where discrete chaotic sequences prevail. In some recent publications, which inspired us for the given investigation, the researchers propose to employ pieces of chaotic waveforms instead of discrete sequences for systems with matched filtering-based demodulation. For example, in (Yao *et al.* 2019), authors have implemented a prototype that demonstrated excellent characteristics of continuous-time chaotic waveforms used in matched-filtering based DCSK communication system. In (Aboltins *et al.* 2022), authors use pieces of orthogonalized chaotic waveforms from continuous-time Chua oscillator model for pre-coding of orthogonal frequency division multiplexing (OFDM) signal. This approach allows improvement in the diversity of OFDM link and the potential use of chaotic synchronization for symbol timing in OFDM. A similar approach with multi-level CSK is used in research (Yang *et al.* 2017).

Communication systems can employ chaotic carrier directly (Sushchik *et al.* 2000; Andreyev 2023) or use up-conversion to the sinusoidal carrier (Jovic 2017). In the case of up-conversion, one of the significant problems of wireless communication systems arises—carrier frequency synchronization. In the case of carrier frequency offset (CFO), the chaotic signal will be modulated by low-frequency harmonic waveform, leading to the loss of chaotic features and substantial change of the waveform. One of the easiest ways to fight with CFO is the use of frequency modulation (FM) on top of chaotic modulation (Cirjulina *et al.* 2022; Hasjuks *et al.* 2022; Yao *et al.* 2019; Ma *et al.* 2022). Since FM is frequently used for mitigation of CFO, in current research, we explore the impact of FM on the BER of chaos-based communication systems.

Chaotic spreading signals or sequences can provide excellent means for code-based multiple access (Sumith Babu and Kumar 2020). The amount of multiple user interference (MUI) primarily depends on cross-correlation among spreading codes at various time delays. Practical experiments of our research group with software-defined radio (SDR) (Aboltins and Tihomorskis 2023) have shown that chaotic synchronization-based have relatively

high MUI due to limited orthogonality among signals from the same chaotic generator with different parameters. Performance analysis of chaotic sequences based code division multiple access (CDMA) system with frequency-selective channel and antenna diversity is presented in (Patel *et al.* 2015b). This paper explores the impact of the synchronization mechanism and quantization on the performance of multi-user chaos-based communication systems.

## SPREAD SPECTRUM MODULATION SCHEMES

### Matched filtering-based chaotic spread spectrum systems

A general block scheme of implemented matched filtering-based SS system is presented in Figure 1. SS system spreads each data bit  $b(t)$  with period  $T_b$ , which is represented by "-1" and "1", with chaos-based spreading sequence  $c(t)$  via multiplication. The entire sequence's period equals  $T_b$ , and one spreading sequence's element is called a chip, which has period  $T_c$ . Spreading sequence inverts when it is multiplied by data bit  $b(t)$  is "-1" and is left intact when data bit  $b(t)$  is "1". Spread signal from the transmitter is then passed through a communication channel that adds additive white Gaussian noise (AWGN)  $\eta(t)$  to the spread signal. Equation (1) describes received signal  $r(t)$  at the input of the receiver in the case of ideal timing synchronization.

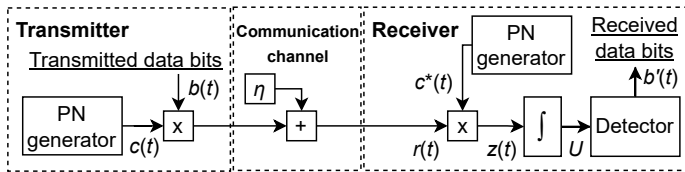


**Figure 1** Block-scheme of baseband matched filtering-based chaotic spread spectrum system

$$r(t) = b(t)c(t) + \eta(t). \quad (1)$$

By adding more users to the channel, each employing a unique spreading sequence  $c_i(t)$  to transmit different data bits  $b_i(t)$ , the received input signal  $r(t)$  from Equation (1) at every user's receiver is defined in Equation (2):

$$r(t) = \sum_{i=1}^n b_i(t)c_i(t) + \eta(t), \quad (2)$$

where  $n$  is the total number of transmitting users in the communication channel.

In the receiver, received signal  $r(t)$  is down-converted and then despread using correlation. This means that received signal  $r(t)$  is multiplied with local spreading sequence  $c^*(t)$  that is the complex conjugate of the sequence  $c(t)$  used in the transmitter, counting in possible delay between the systems, resulting in despread signal  $z(t)$  that is defined in Equation (3):

$$z(t) = r(t)c^*(t) = b(t)c(t)c^*(t) + c^*(t)\eta(t). \quad (3)$$

Multiplying spreading sequence  $c(t)$  by  $c^*(t)$  will produce  $|c(t)|^2$  that is always 1, which means that Equation (3) can be rewritten as Equation (4):

$$z(t) = b(t) + c^*(t)\eta(t), \quad (4)$$

where we can see that signal containing data bits  $b(t)$  is present separately in despread signal  $z(t)$ . In the case of multiple users,

despread signal  $z(t)$  is the combination of  $k$  user's useful data, noise  $\eta(t)$  and additional noise from MAI, i.e. signals from other users, as defined in Equation (5):

$$z_k(t) = b_k(t) + \sum_{\substack{1 \leq i \leq n \\ i \neq k}} b_i(t)c_i(t)c_k^*(t) + c_k^*(t)\eta(t), \quad (5)$$

where  $k$  is the number of a chosen user.

By applying integration to the Equation (4) it is possible to recover data bit  $b(t)$  as shown in Equation (6):

$$U = \int_0^{T_b} b(t) + c^*(t)\eta(t) dt. \quad (6)$$

The threshold detector converts signal  $U$  into received data bits  $b'(t)$ , which compares  $U$  signal's values to "0". Since an ideal timing synchronization is assumed, adjusting the detection point in time is unnecessary.

Classical 2-level DSSS communication system can be implemented as binary phase shift keying (BPSK). BPSK system's BER probability can be expressed via Q-function as Equation (7):

$$P_b = Q\left(\sqrt{2\frac{E_b}{N_0}}\right), \quad (7)$$

where  $P_b$  is probability of an error or theoretical BER,  $E_b$  is energy per bit and  $N_0$  is noise power spectral density. Q is a complementary cumulative distribution function (CCDF) of normal distribution defined as Equation (8):

$$Q(x) = \frac{1}{\sqrt{2\pi}} \int_x^{\infty} e^{-\frac{x^2}{2}} dx. \quad (8)$$

### Chaotic synchronization-based spread spectrum system

Block-scheme of implemented ACSK system (Litvinenko *et al.* 2019), which employs chaotic synchronization for the demodulation, is presented in Figure 2.

ACSK system consists of three chaos generators based on a fourth-order modified Chua's oscillator. One master chaos generator is in the transmitter, whereas two slave chaos generators are in the receiver. Fourth-order modified Chua's oscillator is described by four continuous-time differential equations in Equation (9):

$$\begin{cases} \frac{dp_1}{dt} = -g(p_1, p_3)(p_1 - p_3) - p_2 \\ \frac{dp_2}{dt} = p_1 + \gamma p_2 \\ \frac{dp_3}{dt} = \theta(g(p_1, p_3)(p_1 - p_3) - p_4) \\ \frac{dp_4}{dt} = \sigma p_3 \end{cases}, \quad (9)$$

where  $p_1, p_2, p_3, p_4$  are system's state variables given in Table 1,  $g(p_1, p_3)$  is a piecewise linear function and  $\gamma, \theta, \sigma$  are system coefficients that are given in Table 2.

The difference between generators in the transmitter and receiver is in the absence of piece-wise linear function  $g(p_1, p_3)$  in the receiver's generators that are defined in Equation (10):

$$g(p_1, p_3) = \begin{cases} c(p_1 - p_3 - d) & (p_1 - p_3) > d \\ 0 & (p_1 - p_3) \leq d \end{cases}, \quad (10)$$

where  $c, d$  are system coefficients that are given in Table 2.

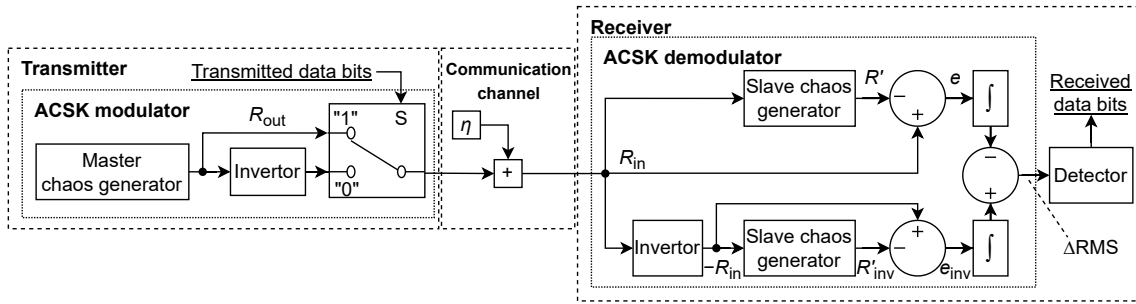


Figure 2 Block-scheme of baseband ACSK system

Table 1 Two ACSK master-slave generator pairs state variables' initial values

User	Master chaos generator (transmitter)				Slave chaos generators (receiver)			
	$p_1$	$p_2$	$p_3$	$p_4$	$p'_1$	$p'_2$	$p'_3$	$p'_4$
1	0.05	0.06	0.07	0.08	0.5	0.6	0.7	0.8
2	0.2386	-2.3058	-0.5283	1.3338	0.2386	-2.3058	-0.5283	1.3338

Table 2 Two ACSK master-slave generator pairs' coefficients of differential equations

User	System coefficients					Weight coefficients			
	$\gamma$	$\theta$	$\sigma$	$c$	$d$	$k_1$	$k_2$	$k_3$	$k_4$
1	0.5	10	1.5	3	1	-2.6302	-0.6054	0.587	0.7763
2	0.25	7	1.4	3	1	-2.0302	-0.2054	1.587	0.0763

In an antipodal modulator, chaotic signal  $R_{out}$  is generated by passing the direct or inverted chaotic signal through the switch, depending on the data bit value. The chaotic signal is inverted when the "0" data bit is spread. The generated chaotic signal at the output of ACSK modulator is expressed in Equation (11):

$$R_{out} = \sum_{i=1}^4 p_i k_i + g(p_1, p_3), \quad (11)$$

where  $p_i$  are system's state variables and  $k_i$  are weight coefficients from Table 2 that define output signal's  $R_{out}$  waveform variation.

In the receiver's ACSK demodulator, two chaotic slave generators are used to synchronize with input signal  $R_{in}$ , one for direct and one for inverted chaotic signal. Chaotic synchronization is a complex phenomenon caused by the trend of the chaotic oscillator settling on a stable orbit if one of the state variables is forced from the outside (Parlitz et al. 1996). Therefore, sufficient conditions for the synchronization are as follows:

- Drive and response systems are similar in terms of stable orbits. Effectively, drive and response systems must have the same design and similar parameters (Cirjulina et al. 2019).
- Signal from the drive to the response system is not distorted too much (Anstrangs et al. 2019) still leads to the same stable orbit.

Using signal  $R_{in}$  as an input for both generators, it is possible to restore piece-wise linear function  $g'(p_1, p_3)$  with additional use of local state variables as shown in Equation (12):

$$g'(p_1, p_3) = R_{in} - \sum_{i=1}^4 p'_i k_i, \quad (12)$$

where  $p'_i$  are slave chaos generators' state variables initialized by values from Table 1. The output signal  $R'$  in Equation (13) is generated similarly to master chaos generator's signal  $R_{out}$  from Equation (11).

$$R' = \sum_{i=1}^4 p'_i k_i + |g'(p_1, p_3)|, \quad (13)$$

where  $|g'(p_1, p_3)|$  is restored piece-wise linear function in absolute form to negate the recovery of incorrect negative values. The calculation of synchronization errors  $e$  and  $e_{inv}$  from both slave chaos generators' output signals  $R'$  and  $R'_{inv}$  is shown in Equation (14):

$$\begin{aligned} e &= R_{in} - R' \\ e_{inv} &= -R_{in} - R'_{inv} \end{aligned} \quad (14)$$

where  $R'$  chaos generators' output signals,  $e$  are chaos generators' synchronization errors and index  $_{inv}$  denotes signals associated

with inverted slave chaos generator. After synchronization errors are obtained, integration is applied for each error, and the difference is calculated in Equation (15):

$$\Delta\text{RMS}(e) = \sqrt{\frac{1}{T_b} \int_{t_n}^{t_n+T_b} [e_{\text{inv}}(t)]^2 dt} - \sqrt{\frac{1}{T_b} \int_{t_n}^{t_n+T_b} [e(t)]^2 dt}, \quad (15)$$

where  $T_b$  is the data bit period in seconds, and  $t_n$  is the time at the moment of calculation in seconds.

This difference  $\Delta\text{RMS}$  is used as an input of an energy detector (Aboltins and Tihomorskis 2023) that detects data bits by calculating the mean value of the whole symbol interval.

### SIMULATION ENVIRONMENT

In this paper, all simulations of the tested communication systems were conducted in MATLAB Simulink environment. The following subsections provide simulated SS systems' descriptions, parameters and visual representation of signals in time and frequency domains.

#### Spread spectrum systems

To be able to compare two different approaches of received signal synchronization in ideal circumstances, two distinct SS systems are implemented: correlation-based DSSS and chaotic synchronization-based ACSK systems. Implemented ACSK system's chaotic signal, which varies in time, spreads data bits according to the description from the previous section.

In previously conducted research (Hasjuks et al. 2022), it was concluded that a predefined signal provides similar performance as a pseudo-noise (PN) generated signal, so in DSSS system PN generator, that was shown in Figure 1, was swapped for the generated signal of a constant number of samples. In total, three different but mutually related spreading signals were generated.

The first signal is a fragment of a master chaos generator recorded output signal  $R_{\text{out}}$  from an ACSK modulator's part before the switch and inverter blocks that were shown in Figure 2. DSSS system employing this signal is named pseudo-chaotic spread spectrum (PCSS), as this signal becomes a discrete periodic signal, repeating a predefined sequence, that is not dependant on any parameters that are used in the generation of the signal in the transmitter.

The second, analogous direct sequence spread spectrum (A-DSSS) system's signal is a continuous-amplitude, discrete-time signal obtained using the Poincare section of the phase portrait created from PCSS signal and its derivative. The resulting signal is up-sampled to the PCSS signal's sample rate.

In the third case, 2-DSSS waveform is obtained by passing A-DSSS signal through a threshold, defined in Equation (16), that selects between two values—"1" and "-1".

$$y_n = \begin{cases} 1 & x_n > \Theta \\ -1 & x_n \leq \Theta \end{cases}, \quad (16)$$

where  $n$  is a signal sample's sequence number,  $y$  is a 2-DSSS signal,  $x$  is an A-DSSS signal before up-sampling and  $\Theta = 0$  is a threshold. After the quantization, the binary 2-DSSS signal is up-sampled to the PCSS and A-DSSS signals' sample rate.

These PCSS, A-DSSS and 2-DSSS signals are used as spreading sequences in a single DSSS system that was modeled in Simulink according to the description from the previous section. None of

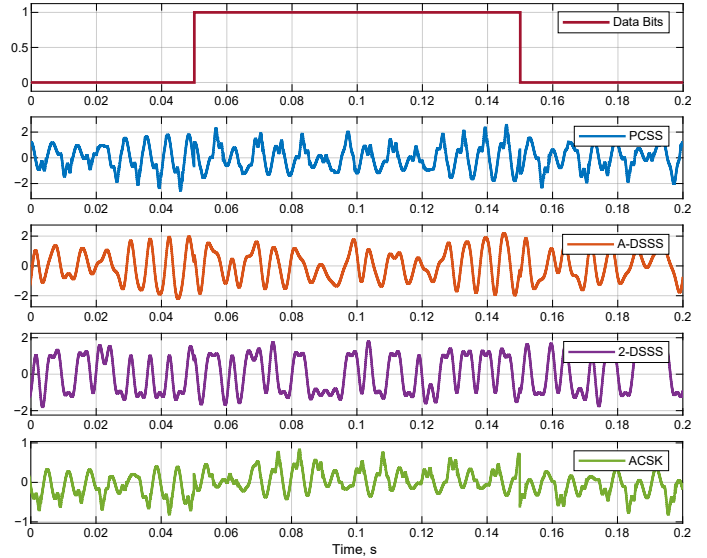


**Figure 3** Baseband signals of chaotic spread spectrum modulations. All spread-spectrum signals have the same bit energy

the parameters of DSSS system are altered after changing between generated SS signals.

SS systems' simulation parameters are compiled in Table 3. Spread data bits using implemented SS systems are presented in Figure 3.

**Table 3** Spread spectrum systems' simulation parameters

Parameter	Value
Data bit frequency $1/T_b$ , Hz	10
Chip frequency $1/T_c$ , kHz	17.05
Spreading sequence's samples per data bit	1705
AWGN channel sample rate, kHz	68.2
Receiver's LPF cut-off frequency, kHz	10

In DSSS system, spreading sequences of defined lengths and values are used. Thus, it is possible to calculate auto and cross-correlations of given sequences. Auto and cross-correlations are presented in Figure 4 and Figure 5, respectively, showing used spreading sequences' correlations. ACSK system's spreading signal is non-repeating, meaning that the signal's auto-correlation and cross-correlation functions are non-constant. Despite this, only at one exact time instant correlation is equal to the PCSS signal's correlation when the spreading sequence was recorded.

As seen from these correlation function figures Fig. 4 and Fig. 5, all signals are related, having similar oscillation patterns at time shifts with varying similarity. It is worth noticing that the correlation function of 2-DSSS decreases more rapidly compared to other systems.

Figure 6 shows the power spectra of the transmitted signals of all compared systems. These systems have similar bandwidth and occupied areas; thus, they can be compared.

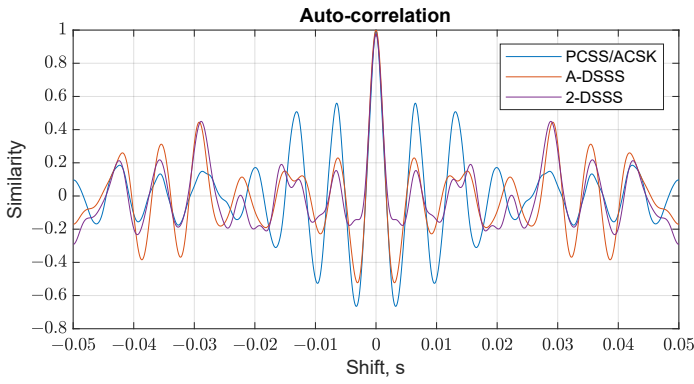


**Figure 4** Auto-correlation function of selected chaotic spreading sequences

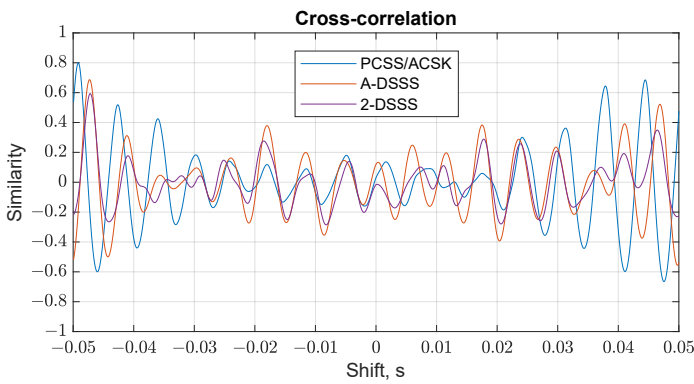


**Figure 5** Cross-correlation between two selected chaotic spreading sequences of the same kind corresponding to different users

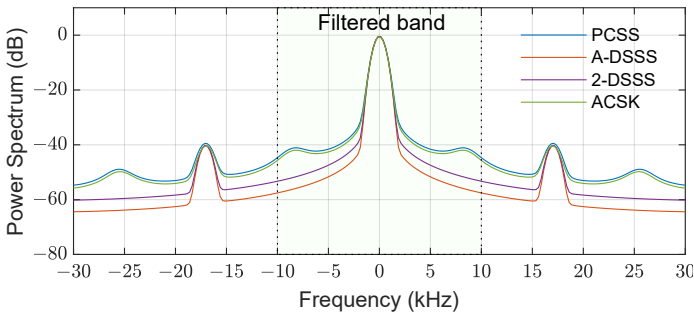


**Figure 6** Power spectra of chaotic spread spectrum systems

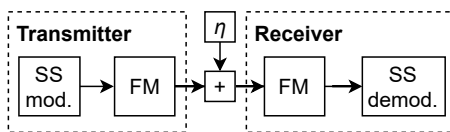


**Figure 7** Block-scheme of frequency modulated spread spectrum systems

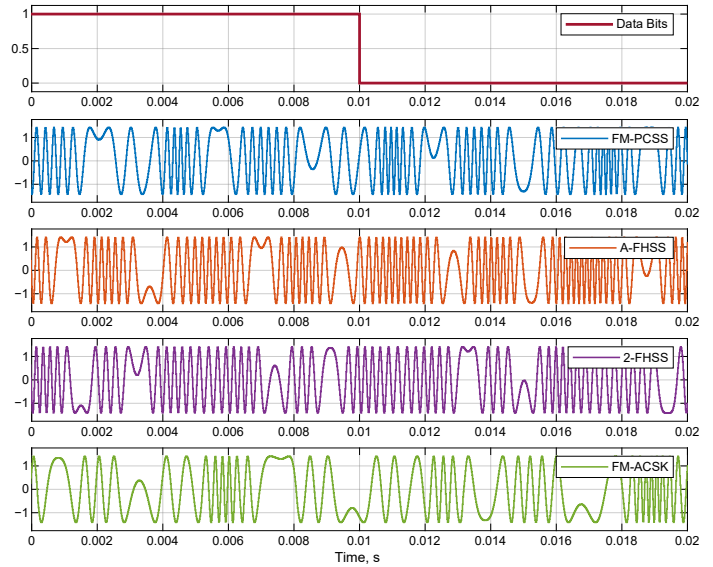


**Figure 8** Baseband signals of frequency-modulated chaotic spread spectrum modulations

Before demodulation, DSSS and ACSK receivers filter incoming signal that was carried through AWGN channel. It is done by using low-pass filter (LPF) that has a cut-off frequency equal to 10 kHz, as marked by the green area labeled "Filtered band" in Figure 6.

### Frequency modulated spread spectrum systems

One of the drawbacks of previously explored direct SS systems is the variable bit energy of the baseband signal. Bit energy can be unified by adding FM after SS modulation in the transmitter, as seen in Figure 7. Moreover, employment of FM significantly eases the practical implementation of the communication system as non-coherent FM does not require precise carrier frequency synchronization as in the case of coherent modulation formats, such as phase shift keying (PSK).

By adding FM to DSSS system, frequency hopping spread spectrum (FHSS) system is created. In FHSS systems, carrier frequency changes between multiple predefined frequencies in some defined order. In this paper, signals employed in FHSS system will be called frequency modulated pseudo-chaotic spread spectrum (FM-PCSS), analogous frequency hopping spread spectrum (A-FHSS) and 2-FHSS, which are FM versions of PCSS, A-DSSS and 2-DSSS signals. ACSK system's FM version is called frequency modulated antipodal chaos shift keying (FM-ACSK).

Simulated FM-SS systems' spread signals are depicted in Figure 8. FM-SS systems have equal bandwidth of  $\approx 10$  kHz and occupy similar area as seen in Figure 9. Comparing spread signals of FM-SS from Figure 8 with direct SS from Figure 3, it can be noted that FM increased the frequency bandwidth of the modulated signals. This is also confirmed by power spectra of FM-SS systems (see Figure 9) are  $\approx 4$  times wider than those of SS systems (see Figure 6), nearly occupying full LPF frequency band until 10 kHz cut-off frequency of receiver's LPF. To achieve equal bandwidth for both FHSS and FM-ACSK systems, different FM deviation values shown in Table 4 were used for each modulation format. In 2-FHSS system, two well-defined peaks at  $\approx 3.6$  kHz are seen, which means that primarily two frequencies are used in spreading, which is also marked in the name of the signal—2-FHSS.

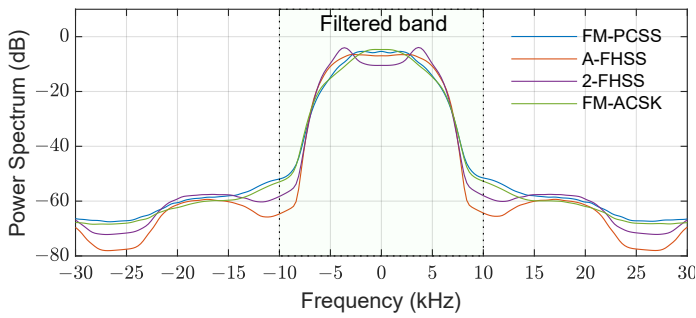


Figure 9 Power spectra of FM-SS systems

Table 4 FM-SS systems' FM deviations

System	FM deviation
FM-PCSS	0.95
A-FHSS	1.05
2-FHSS	3.5
FM-ACSK	7.8

## SIMULATION RESULTS

In this research, three distinct experiments for both SS and FM-SS systems were conducted—data transmission in the single-user scenario, two-user scenario and two-user scenario with receiving user's constant transmitter power and variable transmitter power for interfering user.

### Performance comparison of direct spread-spectrum systems

Results for SS systems in the single-user scenario are presented in Figure 10 and for a two-user scenario in Figure 11. In a two-user scenario, mean BER is provided at the Y-axis, calculated by dividing the sum of both users' BER by 2.

As it can be seen, DSSS system, using any of the previously generated spreading sequences, outperforms ACSK system in both cases. Looking at DSSS system's signals, 2-DSSS outperforms both PCSS and A-DSSS, but PCSS comes in second place, insignificantly surpassing A-DSSS.

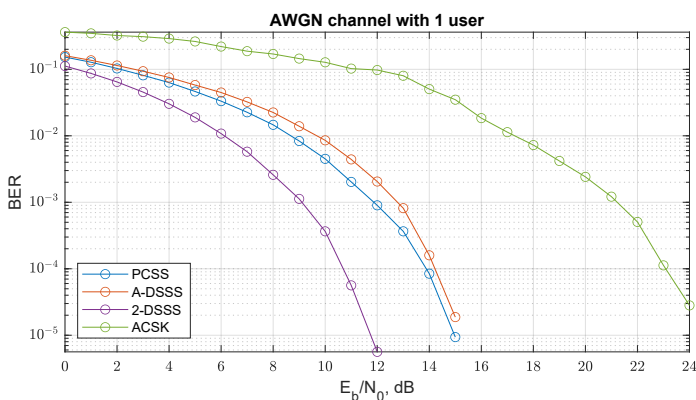


Figure 10 BER versus  $E_b/N_0$  for chaotic spread spectrum systems in single-user scenario

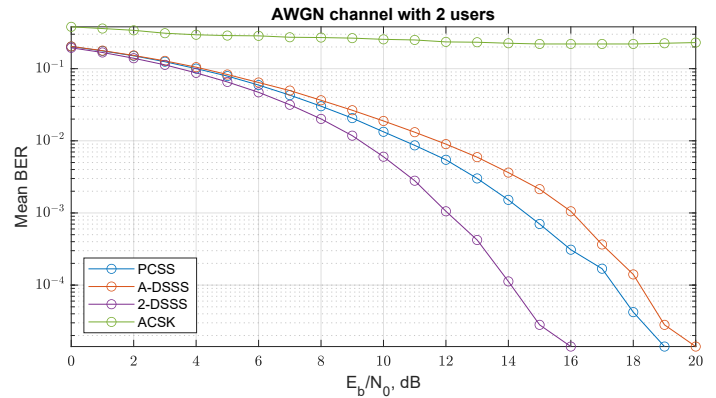


Figure 11 BER versus  $E_b/N_0$  for chaotic spread spectrum systems in two-user scenario

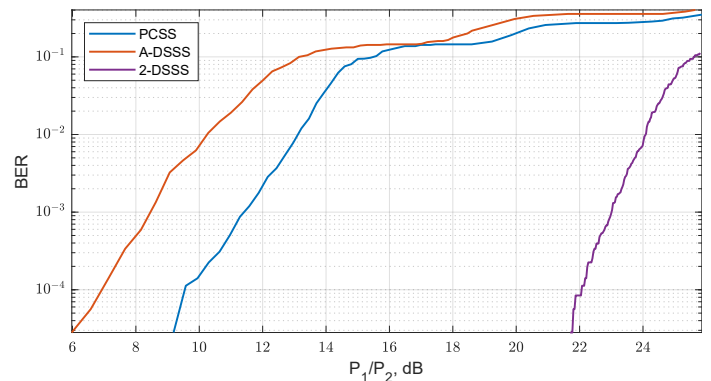


Figure 12 Receiving user's BER versus  $P_1/P_2$  at  $E_b/N_0 = 20$  dB

In the two-user scenario, mean BER results show that communication using two ACSK transmitter/receiver pairs at exactly equal center frequency leads to both users being unable to receive their transmitted data. This means that both ACSK receivers are synchronizing with each user's transmitted signal despite having different initial state conditions and coefficients. In DSSS system, all used signals lead to similar results but lower system performance at equal  $E_b/N_0$  values compared to the single-user scenario.

MUI simulations were carried out, where one of the user's transmitter power  $P_1$  was varied, whereas the receiving user's transmitter power  $P_2$  was constant in all simulations. This power ratio  $P_1/P_2$  is displayed in dB, and the results of these simulations are depicted in Figure 12. The communication channel between the users is noise-free.

These results mirror previously presented results from Figure 11, showing that better performing spreading signal in DSSS also has a better resistance to MAI.

At higher  $E_b/N_0$  or without any noise present in the communication channel, when lowering the interfering transmitter's power, drop from  $BER > 10^{-1}$  to immeasurable BER, at a given number of transmitted data bits, will be instant. To show a gradual decrease in BER, AWGN with  $E_b/N_0 = 20$  dB was used.

### Performance comparison of FM spread-spectrum systems

Results depicted in Figure 13 show that in a single-user scenario, similarly to the direct SS systems, 2-FHSS significantly outperforms other systems. Moreover, the FHSS system employing FM-PCSS signal has slightly worse performance than one using A-FHSS signal. Despite this, with any of the used spreading signals, FHSS

systems manage to outperform FM-ACSK system, but with a more negligible difference of  $E_b/N_0$  between the worst performing FHSS and FM-ACSK, comparing to results of SS systems from Figure 10.

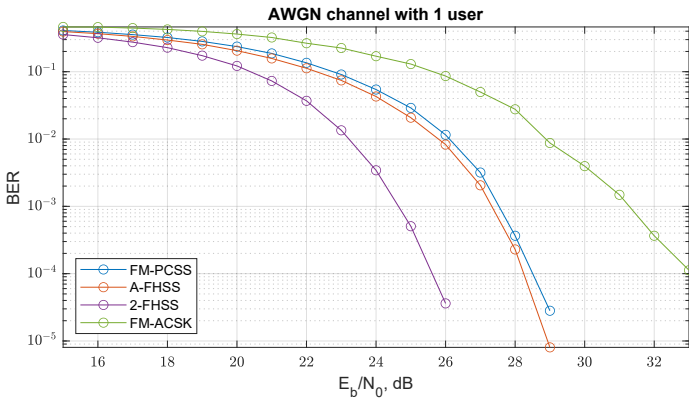


**Figure 13** BER versus  $E_b/N_0$  for FM-SS systems in single-user scenario

In the case of two-user, FHSS system with 2-FHSS spreading signal has a gradual decrease in mean BER, as seen in Figure 14. Both FM-PCSS and A-FHSS signals in FHSS system hit a threshold at  $BER \approx 10^{-6}$  and  $BER \approx 10^{-5}$  respectively. These signals have an equal mean BER at  $E_b/N_0 \leq 27$ , but at  $E_b/N_0 > 27$  employment of FM-PCSS in FHSS system shows an improvement in system's performance over the use of A-FHSS signal. Similarly to the results of ACSK system in the two-user scenario from Figure 11, FM-ACSK system's users can not communicate on the same carrier frequency.

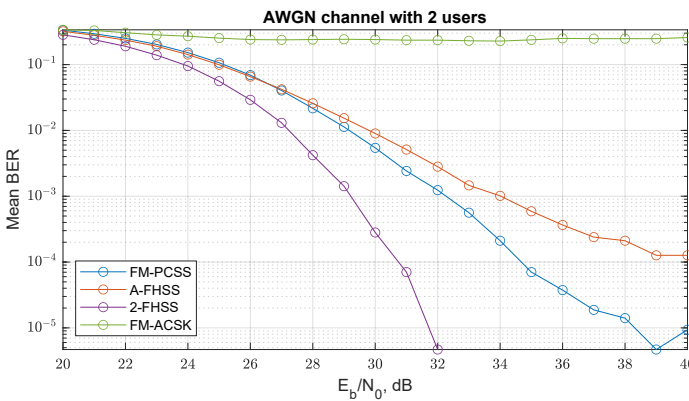


**Figure 14** BER versus  $E_b/N_0$  for FM-SS systems in two-user scenario

In Figure 15 BER versus power ratio  $P_1/P_2$  is shown where  $P_1$  is interfering with the transmitter's power and  $P_2$  is receiving the user's transmitter's power. As in Figure 12, this graph mirrors results previously depicted in Figure 14. Receiving user's BER increases when the interfering transmitter's power increases.

## CONCLUSION

This research aimed to compare matched filtering and chaotic synchronization SS systems. For this purpose, four SS systems were implemented—DSSS, ACSK and their FM variants—FHSS and FM-ACSK. Simulations have shown that DSSS and FHSS systems both outperform ACSK and FM-ACSK systems. In all cases, DSSS and FHSS systems employing binary spreading signal generated

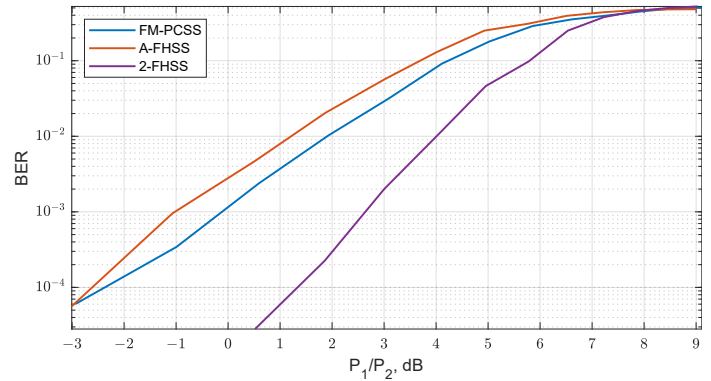


**Figure 15** Receiving user's BER versus  $P_1/P_2$  at  $E_b/N_0 = 30$  dB

by applying a threshold to the quantized version of the recorded sample of the chaotic signal have improved performance over these systems with multi-level spreading signal. In most cases, the continuous-time spreading signal recorded at ACSK master chaos generator's output provided slightly better performance than its sampled version.

As it turns out, the implemented Chua oscillator-based ACSK system can not be used in multi-user scenarios because of malicious synchronization between different users, even with unique parameters of the chaotic oscillator. To solve this problem, chaos generators based on other circuits can be examined. Another solution, as well as potential future research, can be the application of advanced algorithms, including machine learning, to find implemented fourth-order modified Chua's oscillator ACSK chaotic generators' parameter combinations that could prove this ACSK system's usability in a multi-user environment.

In the real application of matched filtering-based systems, the local spreading sequence must be synchronized with the received signal's spreading sequence at a given delayed time, which can be done by the FIR matched filter. ACSK system based on chaotic synchronization, on the other hand, ensures the synchronization of the transmitter's and receiver's chaos generators, which facilitates the development and integration of the chaotic synchronization in the communication systems. Exciting look experiments with ultra-wideband (UWB) pulse synchronization (Chong and Yong 2008; Mesloub et al. 2017; Andreyev 2023), or employment of strongly-quantized signals for the chaotic synchronization.

## Author contributions

Arturs Aboltins designed and supervised the project; Arturs Aboltins developed the concept and designed the methodology; Andreas Ahrens developed the concept; Nikolajs Tihomorskis made the simulations, performed the experiments, visualized results and curated data; Arturs Aboltins validated results; Both Nikolajs Tihomorskis and Arturs Aboltins contributed to the final version of the manuscript.

## Acknowledgments

This work has been supported by the Riga Technical University 2022/2023 project for strengthening scientific personnel capacity Nr. ZM-2023/28, "Implementation of chaos-based data transmission systems in software-defined radio".

## Availability of data and material

The data collected in this study are available from the corresponding author upon reasonable request.

## Conflicts of interest

The authors declare that there is no conflict of interest regarding the publication of this paper.

## Ethical standard

The authors have no relevant financial or non-financial interests to disclose.

## LITERATURE CITED

- Aboltins, A., F. Capligns, N. Hasjuks, and A. Ahrens, 2023 Implementation of chaotic frequency modulation based spread spectrum communication system in software-defined radio. In *IEEE Wireless Communications and Networking Conference, WCNC*, volume 2023-March, pp. 1–6, IEEE.
- Aboltins, A., A. Litvinenko, M. Terauds, and A. Ahrens, 2022 Use of Chaotic Oscillations for Precoding and Synchronization in OFDM. *Advances in Electrical and Electronic Engineering* **20**: 260 – 271.
- Aboltins, A. and N. Tihomorskis, 2023 Software-Defined Radio Implementation and Performance Evaluation of Frequency-Modulated Antipodal Chaos Shift Keying Communication System †. *Electronics (Switzerland)* **12**: 1240.
- Andreyev, Y., 2023 Analytical Model of an Energy Detector for Ultra-Wideband Chaotic Communications. *Electronics (Switzerland)* **12**: 954.
- Anstrangs, D. D., D. Cirjulina, R. Babajans, A. Litvinenko, and D. Pikulins, 2019 Noise Immunity of Chaotic Synchronization in Master-Slave System. In *Advances in Information, Electronic and Electrical Engineering, AIEEE 2019 - Proceedings of the 7th IEEE Workshop*, volume 2019-Novem, pp. 1–5, IEEE.
- Babajans, R., D. Cirjulina, J. Grizans, A. Aboltins, D. Pikulins, *et al.*, 2021 Impact of the Chaotic Synchronization's Stability on the Performance of QCPSK Communication System. *Electronics* **10**: 640.
- Berber, S. M. and A. K. Gandhi, 2016 Inherent diversity combining techniques to mitigate frequency selective fading in chaos-based DSSS systems. *Physical Communication* **19**: 30–37.
- Cai, X., W. Xu, S. Hong, and L. Wang, 2021 A Trinal-Code Shifted Differential Chaos Shift Keying System. *IEEE Communications Letters* **25**: 1000–1004.
- Candido, R., D. C. Soriano, M. T. Silva, and M. Eisenkraft, 2015 Do chaos-based communication systems really transmit chaotic signals? *Signal Processing* **108**: 412–420.
- Chong, C. C. and S. K. Yong, 2008 UWB direct chaotic communication technology for low-rate WPAN applications. *IEEE Transactions on Vehicular Technology* **57**: 1527–1536.
- Cirjulina, D., D. D. Anstrangs, R. Babajans, A. Litvinenko, and S. Tjukovs, 2019 Influence of element nominal values on chaos oscillator dynamics and synchronization. In *Advances in Information, Electronic and Electrical Engineering, AIEEE 2019 - Proceedings of the 7th IEEE Workshop*, volume 2019-Novem, pp. 1–5, IEEE.
- Cirjulina, D., D. Pikulins, R. Babajans, M. Zeltins, D. Kolosovs, *et al.*, 2022 Experimental Study on FM-CSK Communication System for WSN. *Electronics (Switzerland)* **11**: 1517.
- Hasjuks, N., H. Hellbruck, and A. Aboltins, 2022 Performance study of chaos-based DSSS and FHSS multi-user communication systems. In *Proceedings of 2022 Workshop on Microwave Theory and Techniques in Wireless Communications, MTTW 2022*, pp. 23–28, IEEE.
- Hassan, M. F. and M. Hammuda, 2019 A new approach for constrained chaos synchronization with application to secure data communication. *Journal of the Franklin Institute* **356**: 6697–6723.
- Jovic, B., 2017 Class of novel broadband chaos-based coherent communication systems. *IET Communications* **11**: 1970–1984.
- Li, A. and C. Wang, 2017 Efficient Data Transmission Based on a Scalar Chaotic Drive-Response System. *Mathematical Problems in Engineering* **2017**: 1–9.
- Litvinenko, A. and A. Aboltins, 2016 Use of cross-correlation minimization for performance enhancement of chaotic spreading sequence based asynchronous DS-CDMA system. In *2016 IEEE 4th Workshop on Advances in Information, Electronic and Electrical Engineering (AIEEE)*, pp. 1–6, IEEE.
- Litvinenko, A., A. Aboltins, D. Pikulins, A. Ahrens, F. Capligns, *et al.*, 2019 Advanced Chaos Shift Keying Based on a Modified Chua's Circuit. In *2019 IEEE Microwave Theory and Techniques in Wireless Communications (MTTW)*, pp. 17–22, IEEE.
- Liu, F., 2019 Unconventional direct acquisition method for chaotic DSSS signals. *AEU - International Journal of Electronics and Communications* **99**: 293–298.
- Ma, H., Y. Fang, P. Chen, and Y. Li, 2022 Reconfigurable Intelligent Surface-aided M-ary FM-DCSK System: a New Design for Non-coherent Chaos-based Communication. *IEEE Transactions on Vehicular Technology* pp. 1–15.
- Mesloub, A., A. Boukhelifa, O. Merad, S. Saddoudi, A. Younsi, *et al.*, 2017 Chip Averaging Chaotic ON-OFF Keying: A New Non-Coherent Modulation for Ultra Wide Band Direct Chaotic Communication. *IEEE Communications Letters* **21**: 2166–2169.
- Mukherjee, S. and D. Ghosh, 2014 Design and performance analysis of a novel FM-chaos based modulation technique. In *IEEE Wireless Communications and Networking Conference, WCNC*, pp. 594–599, IEEE.
- Parlitz, U. and S. Ergezingler, 1994 Robust communication based on chaotic spreading sequences. *Physics Letters A* **188**: 146–150.
- Parlitz, U., L. Kocarev, T. Stojanovski, and H. Preckel, 1996 Encoding messages using chaotic synchronization. *Physical review. E, Statistical physics, plasmas, fluids, and related interdisciplinary topics* **53**: 4351–4361.
- Patel, M. K., S. M. Berber, and K. W. Sowerby, 2015a Adaptive RAKE receiver in chaos based pilot-added DS-CDMA system. *Physical Communication* **16**: 37–42.
- Patel, M. K., S. M. Berber, and K. W. Sowerby, 2015b Performance Analysis of Adaptive Chaos Based CDMA System with Antenna Diversity in Frequency Selective Channel. *Wireless Personal Communications* **84**: 1439–1448.
- Que, D. T., N. X. Quyen, and T. M. Hoang, 2021 Performance of Improved-DCSK system over land mobile satellite channel under effect of time-reversed chaotic sequences. *Physical Communication* **47**: 101342.
- Quyen, N. X., 2017 On the Study of a Quadrature DCSK Modulation Scheme for Cognitive Radio. *International Journal of Bifurcation and Chaos* **27**: 1750135.
- Sangeetha, M. and V. Bhaskar, 2020 Improved Non-coherent Communication Systems Using Noise Reduction Chaotic ON-OFF Keying (NR-COOK) Techniques. *Wireless Personal Communications* **113**: 1297–1314.
- Sumith Babu, S. B. and R. Kumar, 2020 A High Capacity 1D-Chaotic-Collaborative-CDMA Scheme for Shared Band 5G-IoT Operation. *Wireless Personal Communications* **115**: 307–314.
- Sushchik, M., N. Rulkov, L. Larson, L. Tsimring, H. Abarbanel, *et al.*, 2000 Chaotic Pulse Position Modulation: A Robust Method of Communicating with Chaos. *IEEE Communications Letters* **4**: 128–130.
- Yang, H., W. K. S. Tang, G. Chen, and G.-P. Jiang, 2017 Multi-Carrier Chaos Shift Keying: System Design and Performance Analysis.

IEEE Transactions on Circuits and Systems I: Regular Papers pp. 1–13.

Yao, J. L., Y. Z. Sun, H. P. Ren, and C. Grebogi, 2019 Experimental wireless communication using chaotic baseband waveform. *IEEE Transactions on Vehicular Technology* **68**: 578–591.

Yuan, G., Z. Chen, X. Gao, and Y. Zhang, 2021 Enhancing the Security of Chaotic Direct Sequence Spread Spectrum Communication through WFRFT. *IEEE Communications Letters* **25**: 2834–2838.

Zhang, G., N. Cui, and T. Zhang, 2015 System Based on Walsh Code. *Journal of Electrical and Computer Engineering* **2015**.

**How to cite this article:** Tihomorskis, N., Ahrens, A. and Aboltins, A. Chaotic Spread-Spectrum Communication: A Comparative Study between Chaotic Synchronization and Matched Filtering. *Chaos Theory and Applications*, 6(3), 170-179, 2024.

**Licensing Policy:** The published articles in CHTA are licensed under a [Creative Commons Attribution-NonCommercial 4.0 International License](https://creativecommons.org/licenses/by-nc/4.0/).

